Desalination and Water Treatment
www.deswater.com

doi:10.5004/dwt.2018.22495

115 (2018) 315–325
May

Adsorptive filtration of azo dyes by polysulfone membranes blended with polyaniline based MCM-48 mesopore prepared from rice husk

Y. Tabar, M.R. Toosi*

Department of Chemistry, Qaemshahr Branch, Islamic Azad University, Qaemshahr, Iran, email: yasertabar500@yahoo.com (Y. Tabar), Tel. +981142155050, email: mrtoosi@gmail.com (M.R. Toosi)

Received 1 December 2017; Accepted 13 May 2018

ABSTRACT

MCM-48 was synthesized from rice husk, coated by polyaniline and blended by polysulfone membranes for the removal of azo dyes in batch experiments and dynamic filtration. The blended membranes demonstrated more hydrophilicity and pure water flux (5.8 kg/m^{2}h for non-filled membrane and 413.7 kg/m^{2}h for the sample with 1.2 wt.% of composite). Results showed that the amine groups of polyaniline in the composite played key role in the removal of azo dyes. Dye rejections reached 98% for Reactive Red B (J = 48 kg/m^{2}h), 99% for Blue 62 (J = 29 kg/m^{2}h), and 78% for Yellow GC (J = 12 kg/m^{2}h) in pH = 3, respectively.

Keywords: Azo dyes; MCM-48; Polysulfone; Mixed matrix membrane; Ultrafiltration

1. Introduction

Treatment of wastewater in textile industries is an important subject in order to the large amount of water consumed in these factories, so the recycle of wastewaters after treatment should be economically considered. In addition, environmental pollution due to the formation of hazardous products after degradation of residual dyes by natural reagents is another reason for the importance of treatment of textile wastewaters. Azo dyes are generally used in textile industries, more than 70% of annual dye consumption in the world [1]. Degradation or decomposition of them in wastewater produces several toxic intermediates such as benzene, aromatic amines, and heterocyclic compounds which can lead to serious illnesses in animals and human [2].

Treatment processes for removal of azo dyes from wastewaters can be generally divided to three main categories: (1) Chemical treatments such as chemical/catalytic oxidation [3], flocculation/coagulation [4], and AOP processes by UV, O_3, and/or TiO_2 [5] which are known as high efficient methods for decolorization and too costly in order to the consumption of chemical reagents and detoxification of byproducts after treatment; (2) Biological treatments by enzyme [6], bacteria [7], and fungi [8] as simple methods for design, inexpensive and available but they are mostly large for installation, kinetically slow and very sensitive to the operative parameters such as temperature and pH; (3) Physical methods such as adsorption of residual dyes in effluent by natural or synthetic adsorbents such as activated carbon [9], CNT's [10], alumina [11], zeolites [12], MOF's [13], chitosan [14], clays [15], magnetite [16], etc. in individual form or after surface modification via functionalization by chemical compounds. Most of them demonstrate high adsorption capacity of dyes but the main problem is the separation of adsorbent particles from treated water and prevention of releasing them into the environment.

Filtration by membranes as another physical process can be used for water treatment in large scale and continuous systems. One of the main categories of membrane filtrations is ultrafiltration or nanofiltration by polymeric membranes in order to their high removal efficiency, high flexibility, simple mechanism of pore formation, and simple installation [17]. Mixed matrix membranes (MMM's) as modified polymeric membranes can be prepared by blending

*Corresponding author.

polymer with an inorganic, organic, or composite material during membrane casting. The modifier is added in order to enhance the porosity, permeability, and fouling resistance resulting high efficiency and low energy consumption [18]. Mechanisms of dye rejection during membrane filtration by MMM's are size exclusion, charge exclusion (Donnan effect), and adsorptive filtration. Several literatures have been published about application of MMM's for ultra/nanofiltration of textile dyes. Wrapped MWCNT nanotube was used for fabrication of PES mixed matrix nanofiltration membrane and applied for removal of Acid Orange 7 [19]. It was reported high removal efficiency (more than 99%) in order to the adsorptive mechanism of dyes on the wrapped MWCNT in membrane structure. ZnO/MWCNT nanocomposite was used as a modifier of PES nanofiltration membrane for rejection of Direct Red 16 [20]. The results showed high efficiency (more than 90%) for dye rejection according to Donnan effect. Chitosan/hydroxyapatite/PEG composite membranes were used for dynamic filtration and static adsorption of Direct Blue 15 [21]. Two mechanisms of size exclusion and adsorption of dye over functional groups in membrane were explained. Nanosized ZnO particles were blended into cellulose-acetate-polyurethane membranes for photocatalytic degradation of RR 11 and RO 84 dyes [22]. PVDF nanofiltration membrane mixed by brij-58 was used for RR 141 dye rejection [23]. It was found that the rejection increased by dopant content in membrane in order to increase of membrane hydrophilicity and rate of water molecules to pass through membrane compared with the solute. Carboxymethyl chitosan/Fe_3O_4 nanocomposite was blended by PES membrane for nanofiltration of Direct Red 16 dye solution [24]. The blended membranes showed higher dye rejection in comparison with unfilled PES membrane according to Donnan exclusion mechanism.

Nanosized adsorptive materials can be used for application of "Adsorptive membrane filtration" (AMF) by blending them with the polymer in casting solution. In these membranes, the dominant mechanism is filtration-adsorption and the membranes act as adsorptive filters [25]. Mesoporous silica materials such as MCM-41 and MCM-48 have high surface area and large pore volume which can be used as efficient adsorbents of various compounds [26–28]. Existence of reactive silanol groups on their structure can modify membrane properties via interactions with the polymer [29]. For example, polysulfone membranes mixed by MCM-41 have been applied for separation of CO_2/CH_4[30], CO_2/N_2 [31], and H_2/CH_4 [32] mixtures in order to the enhance of membrane permeability and reduction of resistance to gas flow inside the large channels of mesopore [33].

In recent years, synthesis of adsorbents based MCM's compounds from natural precursors has been interested as a method of green synthesis. In this study, MCM-48 has been synthesized from rice husk as a natural precursor of silica and coated by polyaniline to produce PANi/MCM-48 composite. The composite has been used as a modifier of polysulfone membranes and applied for dynamic filtration and static adsorption of three different types of azo dyes. Effects of various parameters such as time of experiment, PANi/MCM-48 content, and pH of solution on the membrane performance in filtration system or batch experiments have been also investigated.

2. Experimental

2.1. Materials and methods

Rice husk was provided from rice farms in north of Iran. Hydrochloric (36%) and sulfuric acids (98%), sodium hydroxide (99%), cetyl three methyl ammonium bromide (CTAB, 99%), hydroxy propyl cellulose (HPC, 99%), aniline (99%), potassium iodate (99%), and N-methylpyrrolidone (NMP, 99%) were provided from MERCK. Polysulfone (PSf) (MW = 60 kg/mole) was purchased from BASF (Ultrason® S 6010). All steps in experimental procedure were carried out by use of deionized water.

Acid blue 62 (Telon blue RR 01), Reactive Remozal Red B (RR B), and Direct Sirius Yellow GC (Yellow GC) in sulfonate type were provided from Dystar, India. The structures of these eyes are shown in Fig. 1. Molecular diameter and dipole moment of each dye were calculated by quantum optimization using free Gaussian 98 package (RHF method and STO-3G basis set).

In order to characterize prepared MCM-48 samples, BET measurements was conducted for determination of specific surface area, mean pore size, and total pore volume of MCM-48 by means of BELSORP MINI II instrument (BEL Co.). FTIR technique was also used in order to determine functional groups of pure and coated mesopore by 8400s Shimadzu equipment. Crystalline phase and mesoporous structure in MCM-48 and PANi/MCM-48 samples were determined by means of Philips PW800 device with Cu Kα radiation. SEM micrographs of MCM-48, PANi/MCM-48, and membranes were provided by S-4160, Hitachi. XRF analysis was carried out by a Philips PW1480 X-Ray fluorescence for determination of chemical composition of samples. Zeta potentials and surface charges of membrane samples were determined by electro kinetic analyzer (SurrPASS, Anton-Paar, Austria) using streaming potential measurements and Fairbrother-Mastin equation. A Jenway UV-Vis spectrophotometer was used to determine the concentration of dye in solution using calibration curves.

2.2. Preparation of MCM-48 from rice husk

70 g rice husk was carefully washed by water, grinded and then mixed with 500 mL of HCl (1 M), shaken and heated at 80°C for removal of mineral compounds. After two hours, the sample was washed twice, filtered and dried at 110°C. Afterwards, the sample was kept in a furnace at 650°C for 4 h in order to removal of organic compounds and formation of white ash. 4 g of the prepared ash was mixed by 240 mL of NaOH solution (0.145 M). In another vessel 12.12 g CTAB and 2.4 mL of HCl (36% W/W) was mixed by 216 mL water and stirred for 30 min. Two solutions were then mixed and stirred for 12 h. The mixture was then kept in a Teflon-lined autoclave at 100°C for 72 h. Finally, the prepared gel was filtered, washed by acetone and water, dried and then calcined at 600°C for 6 h. XRF analysis and main components of rice husk before and after calcination are listed in Table 1.

2.3. Synthesis of PANi/MCM-48 composite

100 mL of H_2SO_4 solution (1 M) was mixed with 1.14 g potassium iodate. 0.67 g MCM-48 and 0.5 g HPC and stirred

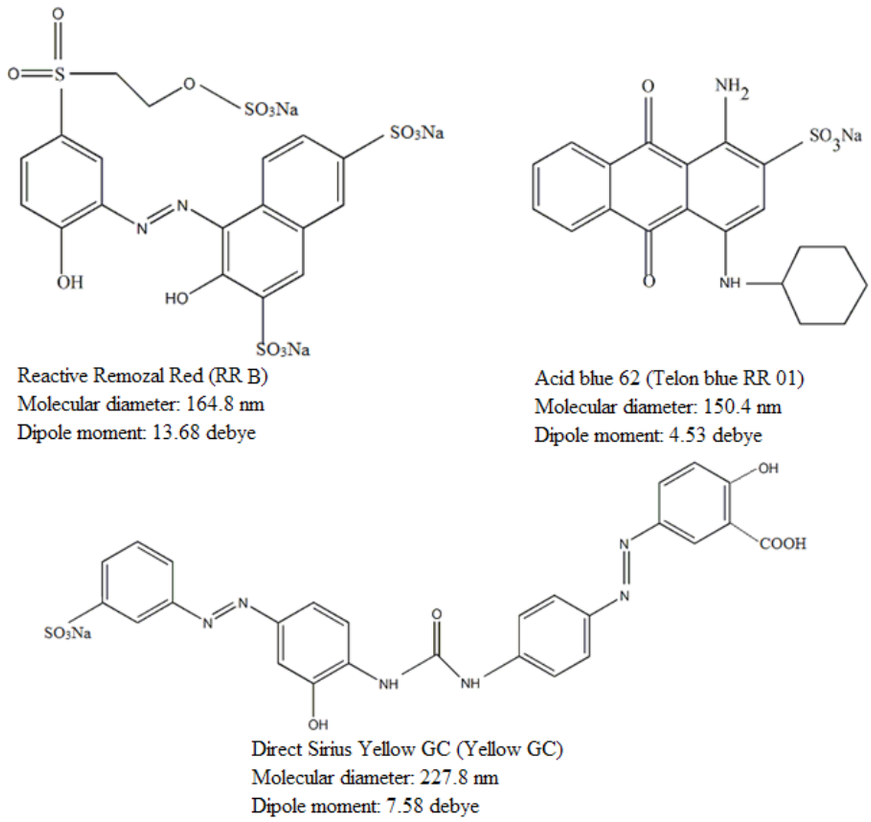

Fig. 1. Details of the used textile dyes.

Table 1
XRF analysis of rice husk before and after calcination

Component	Before calcination, %	After calcination, %
L.O.I	87.97	0.27
SiO_2	11.76	97.88
Al_2O_3	0.08	0.64
K_2O	0.02	0.12
CaO	0.02	0.14
MgO	0.03	0.23
P_2O_5	0.10	0.60
Fe_2O_3	0.01	0.06
Na_2O	0.01	0.06

for 30 min. 0.67 g aniline was then added dropwise to the mixture and stirred for 6 h to appear black color in solution. The solution was then centrifuged and washed by acetone and water several times in order to remove HPC and non-reacted monomers and then dried at room temperature.

2.4. Synthesis of PANi/MCM-48/PSf membrane

Table 2 shows the weight percentage of each component in the casting solution. For each sample, a mixture of NMP and PSf was stirred for 18 h at 60°C. Then, PANi/MCM-48 was added to the solution and stirred again for 8 h to obtain homogeneous mixture of composite in the solution. Afterwards, the casing solution was held at room temperature for 24 h and sonicated for degassing. Membrane synthesis was performed by use of a homemade film applicator on the clean glass by thickness of 150 microns. The glass was immediately immersed into a water bath and kept it for 24 h in order to the extraction of NMP from membrane film. Porosity of membrane was determined by weighting dry and wet samples after dipping in pure water for 24 h by Eq. (1):

$$\varepsilon\ \% = (W - W_0 / \rho A h) \times 100 \quad (1)$$

where W and W_0 are weights of wet and dry membrane, respectively. ρ, A, and h are density of pure water (0.998 g/mL), area (cm^2), and thickness of membrane (cm), respectively.

2.5. Batch sorption experiments

Adsorption of dyes was carried out by use of PANi/MCM-48 powder and the membrane pieces separately in a batch system. 0.1 g of PANi/MCM-48 was added to the 100 mL of dye solution and shaken for 24 h. The solution was then centrifuged to remove PANi/MCM-48 particles and the color of solution was measured by spectrophotometer. For membrane test, 0.1 g of membrane was fragmented to the very small pieces (1 mm × 1 mm), washed by water and

Table 2
Details of properties for the prepared membranes

Membrane	PSF (%)	PANi/MCM-48 (%)	Porosity (%)	PWF (kg/m²h)[a]	Roughness parameters		
					R_a (nm)	R_q (nm)	R_z (nm)
M_0	12.0	0.0	53	5.8	5.26	7.32	55.49
M_1	11.7	0.3	66	118.5	6.98	9.61	67.11
M_2	11.4	0.6	69	234.0	7.67	11.49	141.80
M_3	10.8	1.2	73	413.7	33.66	42.50	191.83

[a]TMP = 2 bar

then added to the dye solution. The experiments were carried out in different values of pH and decolorization was calculated by Eq. (2).

$$R\ (\%) = (1 - C_f/C_i) \times 100 \quad (2)$$

where C_i and C_f demonstrate the initial and final concentrations of dye, respectively.

2.6. Membrane filtration

Filtration experiments were carried out by use of a dead-end flow equipment containing a stainless steel holder (module) with the effective area of 0.0021 m², high pressure pump (2 hp, Pedrollo, Italy), gauge, valves, and water circulating system. Aqueous solution of each dye (C = 100 ppm) was injected to the membrane by pumping at the transmembrane pressure (TMP) of 2 bar and constant temperature of 25°C. After steady state conditions, the flux was determined as:

$$J = m/A{\cdot}\Delta t \quad (3)$$

where m, A, and Δt are the weight of the permeate (kg), effective area of membrane (m²), and time of measurement (s), respectively. Dye rejection for each membrane was calculated by Eq. (4):

$$\text{Rejection}\ (\%) = (1 - C_p/C_f) \times 100 \quad (4)$$

Here, C_f and C_p are dye concentrations in feed and permeate, respectively. All experiments were done at different pH of solution between 3 and 11 for each membrane. Membrane fouling was evaluated by variation of flux and dye rejection by time of filtration.

3. Results and discussion

3.1. Characterization of MCM-48 and PANi/MCM-48 composite

N_2 adsorption-desorption isotherm and diagram of pore size distribution for prepared MCM-48 are given in Fig. 1. The isotherm shows a Langmuir isotherm type IV and hysteresis loop at $P/P_o = 0.9$ indicating capillary condensation on the channels of MCM-48. Maximum of pore size distribution is observed at 1.04 nm and the average pore diameter is 7.309 nm. Specific surface area and total pore volume of MCM-48 are 468 m²/g and 0.912 cm³/g, respectively.

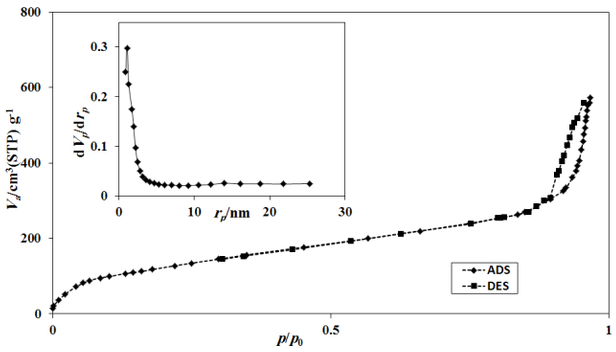

Fig. 2. Diagrams of N_2 adsorption-desorption and pore size distribution of MCM-48.

Fig. 2 shows XRD pattern of prepared MCM-48. The main sharp peak at $2\theta \approx 2.8^o$ corresponds to d_{211} plane as the characteristic peak of MCM-48 indicating formation of mesoporous structure in the sample after calcination [34]. Other weak peaks in 2θ range of 4–6° can be assigned to d_{321}, d_{400}, d_{420}, and d_{332} planes [35].

FTIR spectrums of MCM-48 and PANi/MCM-48 are shown in Fig. 3. The characteristic band of SiO_2 in MCM-48 is asymmetric stretch of siloxane groups appearing as a broad band in 1095 cm^{-1} [36]. It is seen that the intensity of this band reduces in PAN/MCM-48 in order to coverage of mesopore surface by polyaniline chains. Another broad band in spectra of MCM-48 appears in 3400 cm^{-1} corresponded to the stretching band of silanol groups in surface of MCM-48. It can be seen that the intensity of this band in PANi/MCM-48 sample increases remarkably in order to overlap with the stretching band of –NH groups in polyaniline. Vibrational band in 1580 cm^{-1} can be assigned to the C-C stretching band of quinoid rings in polyaniline [37].

SEM micrographs of MCM-48 and PANi/MCM-48 are shown in Fig. 4. It is seen that the particles of mesopore have flaked shape and nanosized particles of polyaniline are carefully dispersed over surface of mesopore in PANi/MCM-48.Presence of the surfactant (HPC) in the mixture prevents coagulation of the polymer chains during polymerization and provides stable colloidal dispersion of polymer particles on MCM-48 [38]. Carefully dispersion of polyaniline over MCM-48 provides large amounts of active sites that can interact with membrane matrix during casting processand enhance membrane properties.

3.2. Characterization of membranes

SEM micrographs of prepared membranes are given in Fig. 5. It is seen that the blended membranes have thinner skin layer and larger finger-like macrovoids in sub-layer in comparison with the non-filled membrane. The macrovoids grow along the sub-layer part of membrane and create asymmetric structure in cross section of membrane. It is clear that the larger pore size and macrovoids increase the permeability of membrane.

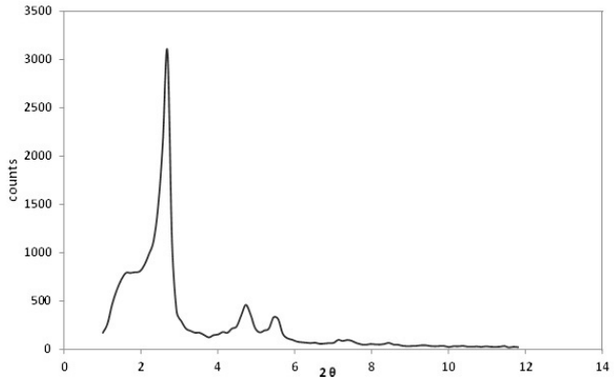

Fig. 3. XRD pattern of prepared MCM-48.

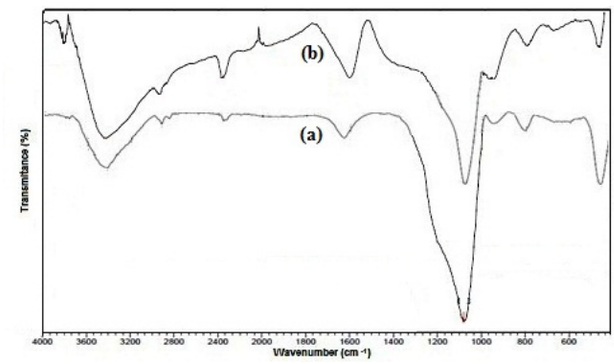

Fig. 4. FTIR spectrums of MCM-48 (a) and PANi/MCM-48 (b).

Fig. 6 shows distribution of PANi/MCM-48 particles in top and cross section of the blended membrane (M_3). It is seen that the particles of composite are dispersed on the membrane surface with the different sizes. From cross section images, the particles of PANi/MCM-48 are also dispersed in the pores and membrane matrix.

Fig. 7 shows zeta potentials of the membranes in different values of pH. It is observed that by increase of PANi/MCM-48 content the zeta potential decreases and iso-electric point (i.e.p) reduces from pH ≈ 8 for M_0 to pH ≈ 5.7 for M_3. Existence of polar amine groups in membrane surface increases negative charge and enhances membrane hydrophilicity resulting better diffusion of water molecules and higher water flux. From Table 2, increase of PANi/MCM-48 content in membrane structure leads to an increase of the porosity in order to the formation of thinner skin layer and larger porous sublayer and macrovoids in the blended membranes.

Fig. 8 demonstrates three dimensional AFM micrographs of membranes. From details of roughness parameters given in Table 2, it is seen that by increase of PANi/MCM-48 content the roughness of membrane increases from R_a = 5.26 nm in M_0 to R_a = 33.66 nm in M_3. It can be resulted from this fact that by addition of PANi/MCM-48 as a polar modifier the rates of phase inversion and precipitation during membrane casting increase. In other words, the higher interfacial interactions and faster replacement of solvent (NMP) and non-solvent (water) in presence of hydrophilic particles of PANi/MCM-48 are observed. So, water molecules can pass through the membrane faster during phase inversion and more pores will be formed in membrane, resulting rougher surface [25]. It is clear that rougher surface provides more effective area for active sites interacting with permeate and enhances diffusion of water molecules.

3.3. Batch experimental results

Details of dyes adsorption over PANi/MCM-48 particles in different values of pH are given in Fig. 9. It is

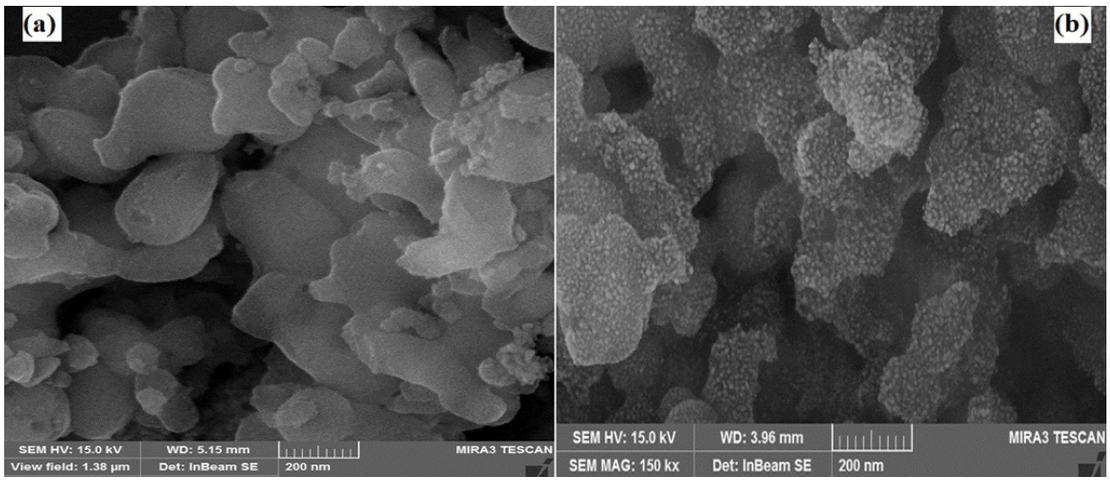

Fig. 5. SEM micrographs of MCM-48 (a) and PANi/MCM-48 (b).

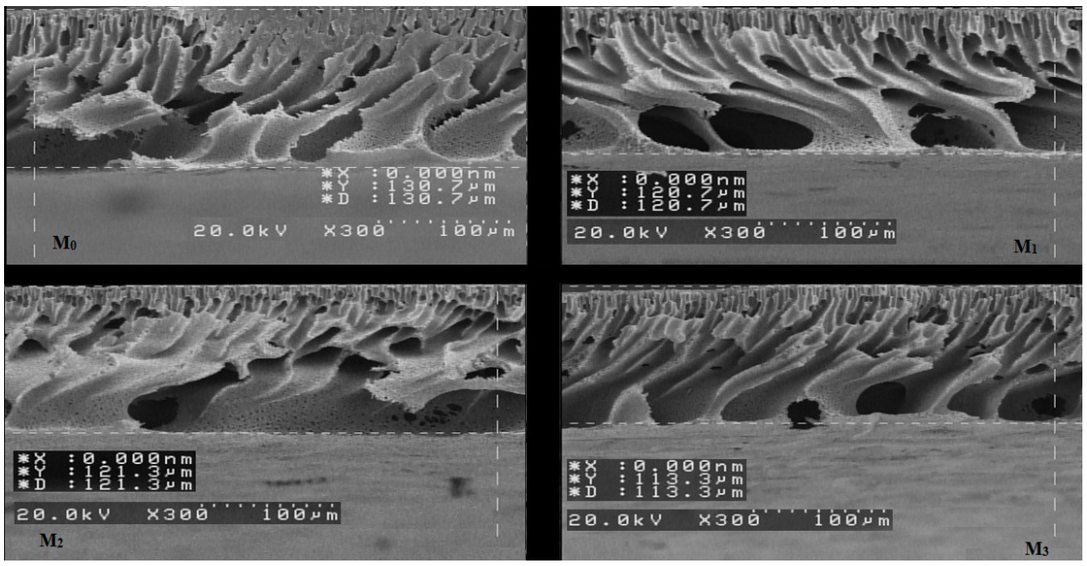

Fig. 6. SEM micrographs of M_0 (a), M_1 (b), M_2 (c), and M_3 (d) membranes.

Fig. 7. SEM images of top surface (a) and cross section (b and c) of M_3.

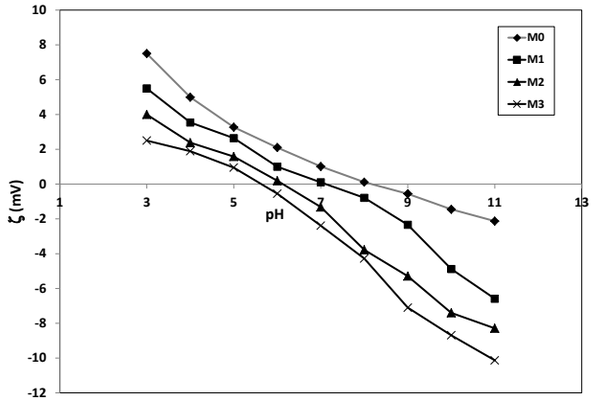

Fig. 8. Zeta potentials of the membranes in different pH.

observed that the adsorption of dyes increases by decrease of pH. It can be related to the dipole moment of dye and interactions between an ionic sulfonate groups in dye and amine groups of PANi/MCM-48 particles. In acidic conditions, the amine groups can be protonated and changed into $–NH_2^+$ species. Therefore, strong interactions between these positive sites and negative sites in dye molecules lead to increase the adsorption. In addition, RR B has larger dipole moment (μ = 13.68 debye) so more adsorption of RR B molecules by interactions with $–NH_2^+$ species in acidic conditions is predictable. On the other hand, the negatively-charged amine groups are formed by increase of pH so the strength of interactions between dye molecules and PANi/MCM-48 particles reduces. It is also observed that the decolorization of Yellow GC solution is lower than the others. It may be related to the biggest size of Yellow GC (227.8 nm) that can limit the rate of diffusion of dye molecules and reduce their interactions with PANi/MCM-48 particles.

Fig. 10 demonstrates the effect of pH on the removal efficiency of dyes by different membranes. It is observed that the removal efficiency is lower than the adsorption by PANi/MCM-48 powder. It can be explained according to the lower mass transfer and diffusion rate of dye molecules onto the membrane and smaller effective surface area of membrane pieces in comparison with PANi/MCM-48 powder. Moreover, the adsorption behavior of dyes on the membranes is different with the PANi/MCM-48 powder. It is observed that the removal efficiency for PANi/MCM-48 powder reduces by increase of pH while

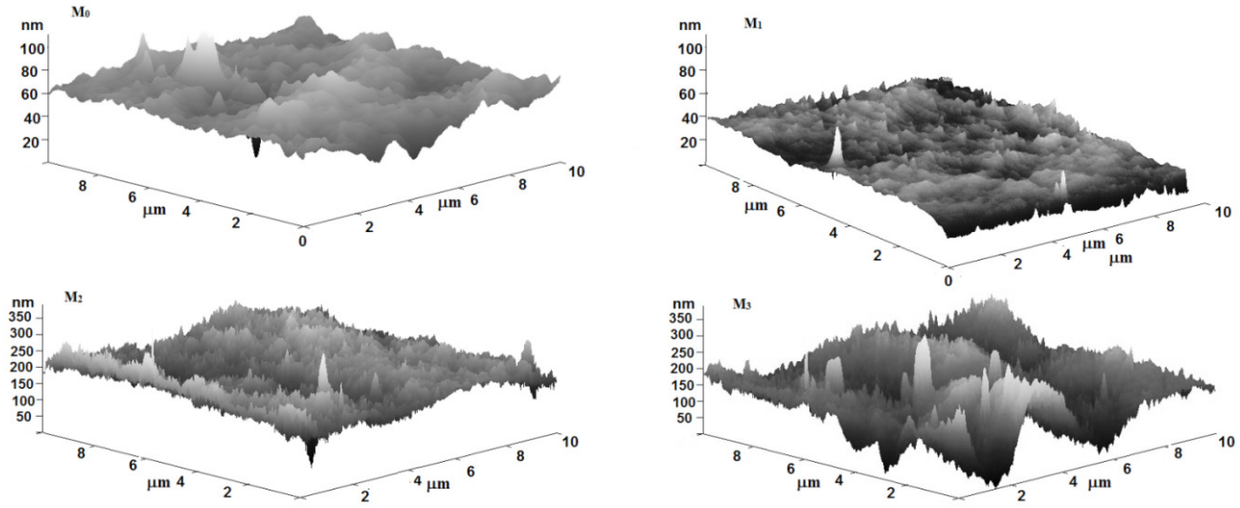

Fig. 9. 3D AFM micrographs of membranes.

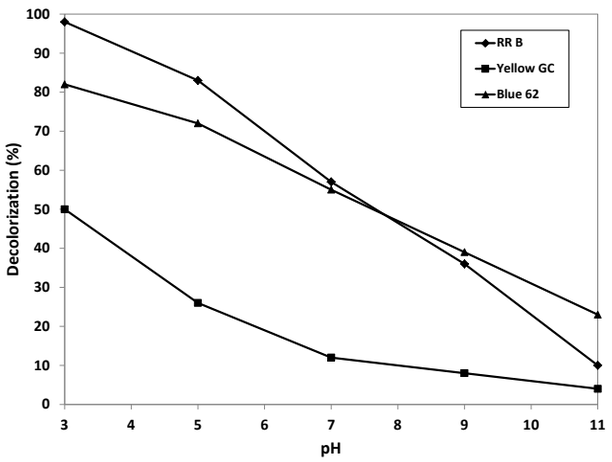

Fig. 10. Removal efficiency of dyes by adsorption on PANi/MCM-48 particles in different pH of solution.

the adsorption by the membrane pieces increases again in pH values higher than 7.Mechanism of adsorption on the membrane can be explained according to the existence of two adsorptive sites: 1) PANi/MCM-48 particles dispersed in the membrane surface/pores and 2) functional groups in polysulfone.

As discussed before, higher adsorption of dye molecules in acidic solutions can be related to the creation of positive sites of $–NH_2^+$ and their interactions with the anionic sites of dye molecules. So, it is predictable that the decolorization in acidic solutions increases by increase of PANi/MCM-48 content in the blended membrane. In addition, sulfonyl groups in membrane can also interact by dye molecules. It was observed (not shown here) that the color of non-filled membrane pieces changed after dye adsorption. The nature of this interaction is not clear but it may be discussed according to the electrostatic attractions between $–SO_2–$ groups in polysulfone and some functional groups in dye molecules such as –NH, $–NH_2$, –COOH, and –N=N– groups. So, the adsorption of dye molecules by sulfonyl groups in the membrane leads to an increase of the decolorization in the basic conditions. It can be also mentioned that the smaller dipole moment of blue 62 and smaller size of Blue 62 increase its adsorption on the membrane pieces more than the others.

3.4. Dynamic filtration results

Results of dynamic filtration by the membranes in different values of pH are given in Fig. 11. It is observed that there are some differences and similarities between the results of dye rejection by filtration and removal by adsorption with the membranes:

1) Removal efficiency of the dyes by membrane filtration is remarkably higher than the batch experiments by membrane pieces. For example, maximum values of removal efficiency for RR B, Yellow GC and Blue 62 by adsorption on M_3 are 25, 29, and 71% in pH = 3 while the rejections of these dyes in similar pH are 98, 78, and 99%, respectively. It can be mentioned to this fact that during filtration process more amount of solution can pass through the membrane by pumping, so the feed solution diffuses more into the membrane and larger number of dye molecules can be adsorbed on the active sites of PANi/MCM-48. From Fig. 11, dye rejection increases by PANi/MCM-48 content in the membrane in order to the larger amounts of active sites in membrane structure.
2) Rejections of dye solutions decrease by increase of pH in neutral conditions and rise again in basic solutions. This behavior is in agreement with the surface charges and zeta potentials of membrane surface. From Fig. 7, by increase of pH surface charges of the membranes are negative and repulsion forces

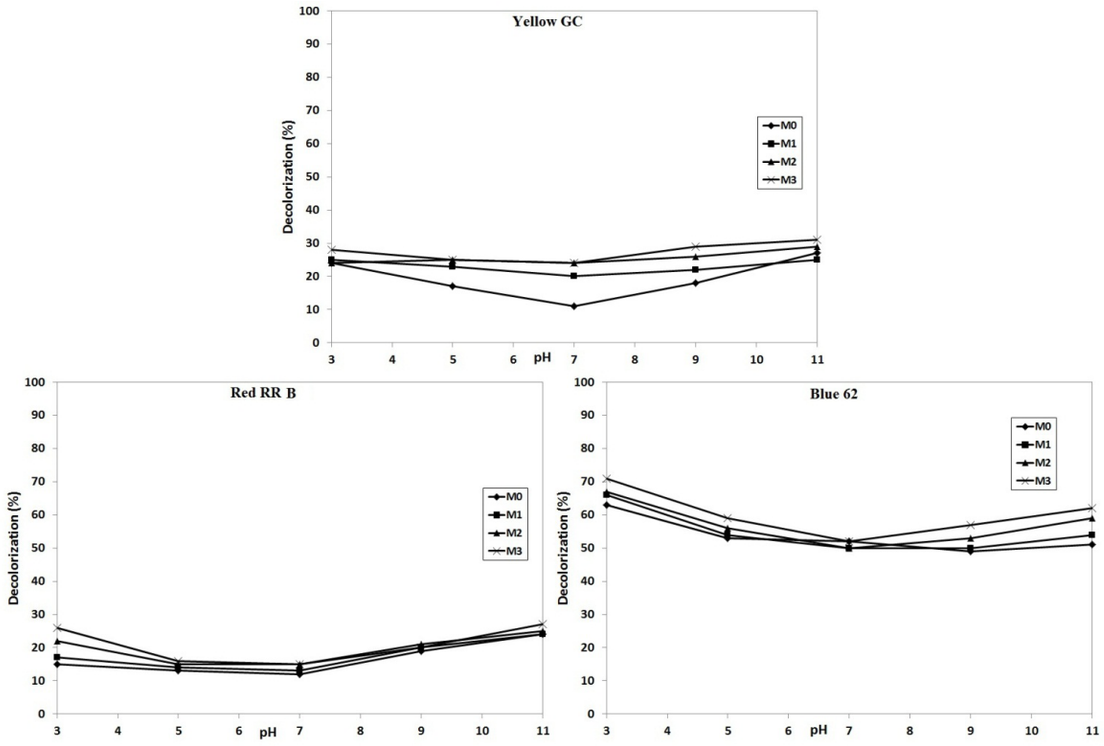

Fig. 11. Removal efficiency of dyes by adsorption on the membranes vs. pH.

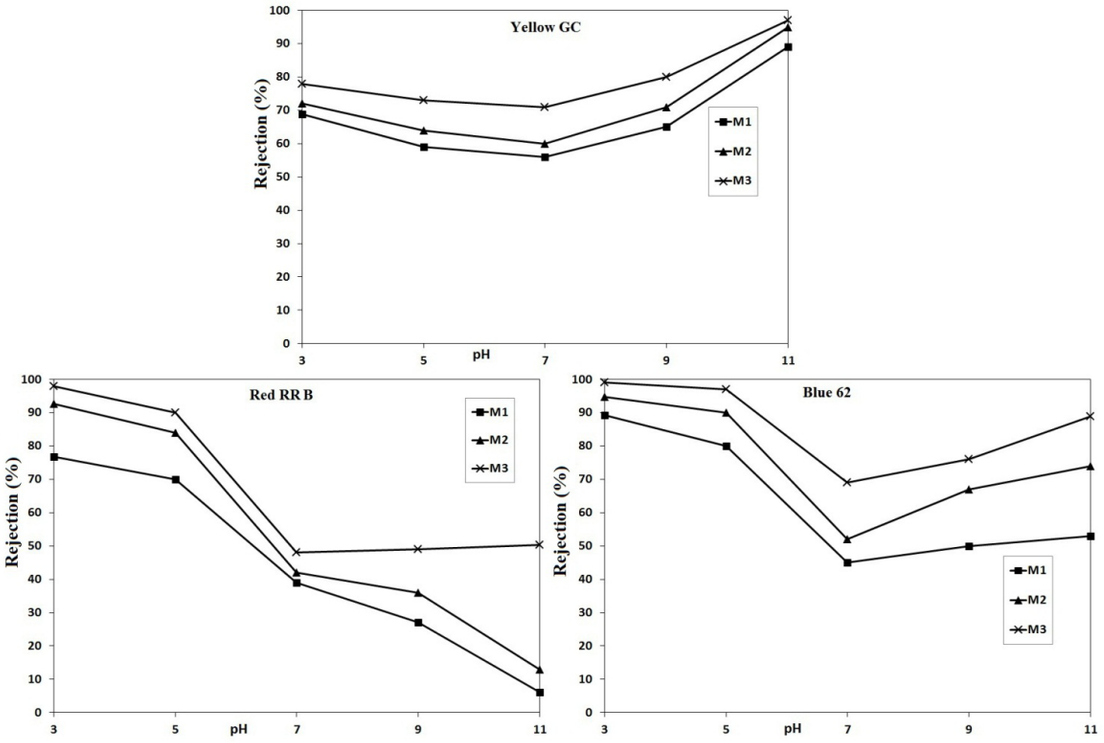

Fig. 12. Rejection of dyes by membrane filtration vs. pH.

between negatively-charged amine groups of PANi/MCM-48 particles and anionic sites of dye molecules increases dye rejection according to Donnan effect. It should be noticed that the rejection in basic solutions becomes more complicated than acidic conditions. For example, while the rejections of Yellow GC and Blue 62 by all membranes increase in basic conditions, RR B solution shows different behavior in filtrations by M_1 and M_2. It may be resultant of charge exclusion effects and complex interactions between functional groups of dyes and sulfonyl groups of polymer in basic solutions discussed in section 3.3. However, it can be concluded that in the membrane with PANi/MCM-48 content more than 1.2 wt.% the dominant mechanism of dye rejection in basic solution is Donnan effect.

Table 3 shows flux and rejection results for some azo dyes by different mixed matrix membranes. It can be seen that the PSf membranes mixed by PANi/MCM-48 particles present remarkable values of flux and azo dyes rejections comparable with the other mixed matrix membrane.

3.5. Membrane fouling

Fig. 12 shows the variations of flux and rejection by time of filtration. Minimum and maximum fluxesare observed in filtration of yellow GC and red RR B solutions, respectively. Decrease of flux by time of filtration can be explained according to the adsorption and fixation of dye molecules on the active sites of membrane resulting blockage of membrane pores. In addition, it is observed that the reduction of flux increases by PANi/MCM-48 content in the blended membranes. For example, flux ofred RR B solution in filtration by M_1 decreases from 35 to 28 kg/m^{2}h (STD = 2.6) after 210 min while it reduces from 41 to 32 (STD = 3.3) and 48 to 35 kg/m^{2}h (STD = 4.8) for M_2 and M_3, respectively. Increase of modifier in membrane matrix leads to adsorb larger number of dye molecules and block more membrane pores.

4. Conclusion

MCM-48 mesopore prepared from rice husk as a natural silica source was coated by polyaniline to prepare a hydrophilic modifier of polysulfone membranes. Results indicated that the blended membranes showed higher permeability and water flux in order to the increase of porosity and hydrophilicity of membranes. Details for adsorption of azo dyes by PANi/MCM-48 particles verified that interactions between amine groups and anionic sites of dye molecules played key role in adsorption of azo dyes. It was also observed that protonation of –NH groupsof polyaniline in PANi/MCM-48 particles increased adsorption of dyes with higher dipole moment and smaller size.

Removal of dyes by use of the membranes in batch experiments showed that the adsorption of dyes was performed by PANi/MCM-48 particles dispersed in membrane matrix in acidic solutions and sulfonyl groups of PSf in basic conditions. Protonated amine groups of PANi/MCM-48 particles in acidic conditions played the key role for dye adsorption while the interactions between functional groups of dyes and sulfonyl groups in PSf was the dominant mechanism of dye removal in basic solutions. Smaller dipole moment enhanced adsorption of dye molecules on the membranes.

Results of dye rejection in dynamic filtration indicated that the blended membranes acted as adsorptive filtration membrane for removal of azo dyes in acidic conditions. Positively-charged amine groups of PANi/MCM-48 particles in membrane could interact with negative sites in dye molecules. By increase of pH, charge exclusion according

Table 3
Comparison of azo dyes rejection with the various types of MMM's

Azo dye	Membrane	Filler/modifier	J_{max} (kg/m^{2}h)	Rejection (%)	Ref.
Direct Blue 15	PEG	chitosan/hydroxyapatite	NA	98	[21]
Reactive Red 141	PVDF	brij-58	31.2	90	[23]
Direct Red 16	PES	chitosan/Fe_3O_4	36	99	[24]
Acid Yellow 17	PSf	phenylene diamine	31.14	93	[39]
Reactive Red 120	PSf	PVP/PANi	55	99	[40]
Acid Blue 193	PES	acrylate/alumoxane	19[a]	96	[41]
Direct Red 28	PVDF	NH_2- halloysite NT	30	94.9	[42]
Direct Red 28	PVDF	dopamine- halloysite NT	42.2	86.5	[43]
Direct Yellow 4	PVDF	dopamine- halloysite NT	42.2	85	[43]
Direct Blue 14	PVDF	dopamine- halloysite NT	42.2	93.7	[43]
Reactive Red 49	PES	halloysite NT	73	90	[44]
Reactive Red B	PSf	PANi/MCM-48	48	98[b]	This work
Acid Blue 62	PSf	PANi/MCM-48	29	99[b]	This work
Direct Yellow GC	PSf	PANi/MCM-48	12	78[b]	This work

[a]in terms of kg/m^{2}h bar
[b] at pH = 3

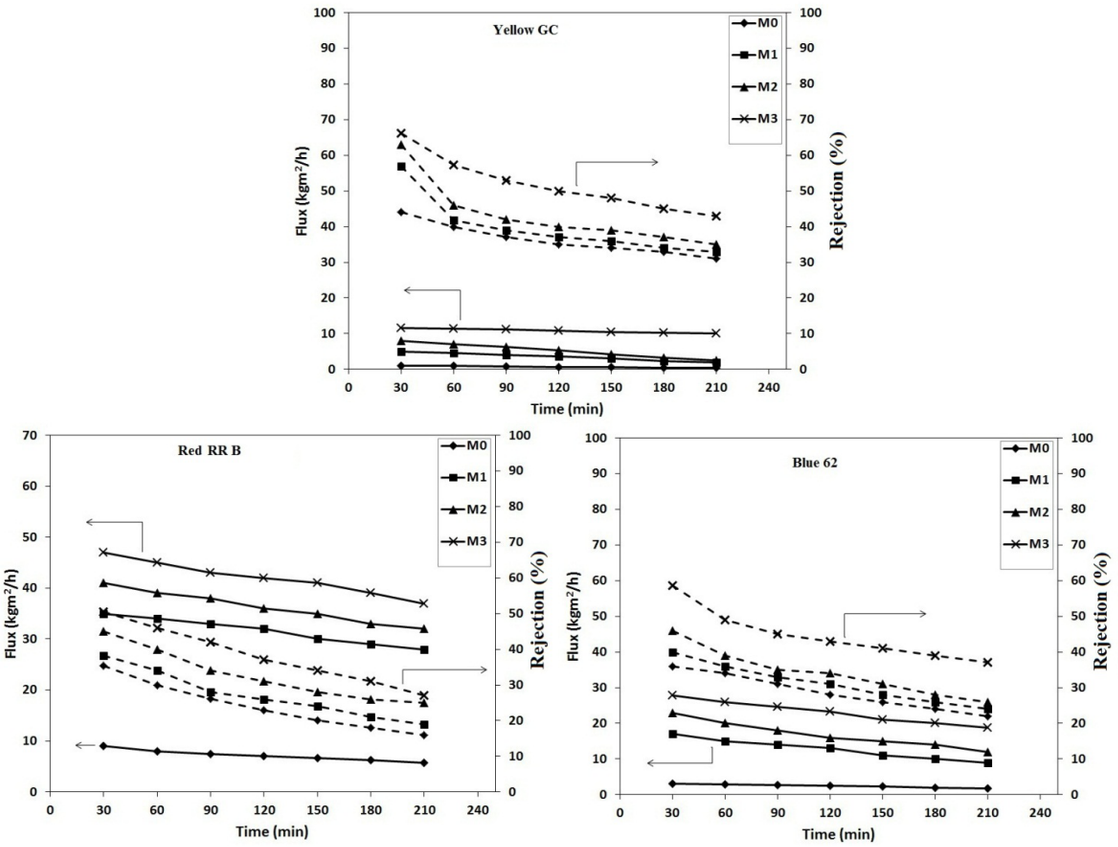

Fig. 13. Variation of permeate flux and rejection by time of filtration.

to the repulsive forces between negatively-charged species and anionic sites in dye molecules was dominant mechanism for dye rejection.

References

[1] K. Balapure, N. Bhatt, D. Adamwar, Mineralization of reactive azo dyes present in simulated textile waste water using down flow microaerophilic fixed film bioreactor, Bioresour. Technol., 175 (2015) 1–7.

[2] D. Rawat, V. Mishra, R.S. Sharma, Detoxification of azo dyes in the context of environmental processes, Chemosphere 155 (2016) 591–605.

[3] M.S. Morsi, A.A. Al-Sarawy, W.A. Shehab El-Dein, Electrochemical degradation of some organic dyes by electrochemical oxidation on a Pb/PbO_2 electrode, Desal. Water Treat., 26 (2011) 301–308.

[4] Y.Y. Lau, Y.S. Wong, T.-T. Teng, N. Morad, M. Rafatullah, S.-A. Ong, Coagulation-flocculation of azo dye Acid Orange 7 with green refined laterite soil, Chem. Eng. J., 246 (2014) 383–390.

[5] W.F. Khalik, S.-A. Ong, L.-N. Ho, Y.-S. Wong, N. A.Yusoff, F. Ridwan, Evaluation on the molecular structure of azo dye in photocatalytic mineralization under solar light irradiation, Desal. Water Treat., 55 (2015) 2229–2236.

[6] R.L. Singh, P.K. Singh, R.P. Singh, Enzymatic decolorization and degradation of azo dyes – A review, Int. Biodeterioration Biodegradation, 104 (2015) 21–31.

[7] R.G. Saratale, G.D. Saratale, J.S. Chang, S.P. Govindwar, Bacterial decolorization and degradation of azo dyes: A review, J. Taiwan Inst. Chem. Eng., 42 (2011) 138–157.

[8] S.K. Sen, S. Raut, P. Bandyopadhyay, S. Raut, Fungal decolouration and degradation of azo dyes: A review, Fungal Biol. Rev., 30 (2016) 112–133.

[9] G.M.D. Ferreira, M.C. Hespanhol, J. de Paula Rezende, A.C. dos Santos Pires, L.V.A. Gurgel, Adsorption of red azo dyes on multi-walled carbonnanotubes and activated carbon: A thermodynamic study, Colloids Surf. A Physicochem. Eng. Asp., 529 (2017) 531–540.

[10] A.K. Mishra, T. Arockiadoss, S. Ramaprabhu, Study of removal of azodye by functionalized multi walled carbon nanotubes, Chem. Eng. J., 162 (2010) 1026–1034.

[11] M. Wawrzkiewicz, M. Wiśniewska, A. Wołowicz, V. M.Gun'ko, V.I. Zarko, Mixed silica-alumina oxide as sorbent for dyes and metal ions removal from aqueous solutions and wastewaters, Microporous Mesoporous Mater., 250 (2017) 128–147.

[12] N. Mirzaei, H.R. Ghaffari, K. Sharafi, A. Velayati, G. Hoseindoost, S. Adabi, A.H. Mahvi, A. Azari, K. Dindarloo, Modified natural zeolite using ammonium quaternary based material for Acid red 18 removal from aqueous solution, J. Environ. Chem. Eng., 5 (2017) 3151–3160.

[13] A. Ayati, M.N. Shahrak, B. Tanhaei, M. Sillanpää, Emerging adsorptive removal of azo dye by metal–organic frameworks, Chemosphere, 160 (2016) 30–44.

[14] A. Szyguła, E. Guibal, M. Ruiz, A.M. Sastre, The removal of sulphonated azo-dyes by coagulation with chitosan, Colloids Surf. A. Physicochem. Eng. Asp., 330 (2008) 219–226.

[15] A. Nejib, D. Joelle, A. Fadhila, G. Sophie, T.-A. Malika, Adsorption of anionic dye on natural and organophilic clays: effect of textile dyeing additives, Desal. Water Treat., 54 (2015) 1754–1769.

[16] Z. Xu, W. Li, Z. Xiong, J. Fang, Y. Li, Q. Wang, Q. Zeng, Removal of anionic dyes from aqueous solution by adsorption onto amino-functionalized magnetic nanoadsorbent, Desal. Water Treat., 57 (2016) 7054–7065.

[17] A.W. Mohammad, Y.H. Teow, W.L. Ang, Y.T. Chung, N. Hilal, Nanofiltration membranes review: Recent advances and future prospects, Desalination, 356 (2015) 226–254.
[18] J. Yin, B. Deng, Polymer-matrix nanocomposite membranes for water treatment, J. Membr. Sci., 479 (2015) 256–275.
[19] N. Ghaemi, S.S. Madaeni, P. Daraei, H. Rajabi, T. Shojaeimehr, F. Rahimpour, B. Shirvani, PES mixed matrix nanofiltration membrane embedded withpolymer wrapped MWCNT: Fabrication and performance optimization in dye removal by RSM, J. Hazard. Mater., 298 (2015) 111–121.
[20] S. Zinadini, S. Rostami, V. Vatanpour, E. Jalilian, Preparation of antibiofouling polyethersulfone mixed matrix NF membrane using photocatalyticactivity of ZnO/MWCNTs nanocomposite, J. Membr. Sci., 529 (2017) 133–141.
[21] C. Shi, C. Lv, L. Wu, X. Hou, Porous chitosan/hydroxyapatite composite membrane for dyes static and dynamic removal from aqueous solution, J. Hazard. Mater., 338 (2017) 241–249.
[22] A. Rajeswari, S. Vismaiya, A. Pius, Preparation, characterization of nano ZnO-blended cellulose, acetate-polyurethane membrane for photocatalytic degradation of dyes from water, Chem. Eng. J., 313 (2017) 928–937.
[23] N. Nikooe, E. Saljoughi, Preparation and characterization of novel PVDF nanofiltration membranes with hydrophilic property for filtration of dye aqueous solution, Appl. Surf. Sci., 413 (2017) 41–49.
[24] S. Zinadini, A.A. Zinatizadeh, M. Rahimi, V. Vatanpour, H. Zangeneh, M. Beygzadeh, Novel high flux antifouling nanofiltration membranes for dye removal containing carboxymethyl chitosan coated Fe_3O_4 nanoparticles, Desalination, 349 (2014) 145–154.
[25] N. Ghaemi, S.S. Madaeni, P. Daraei, H. Rajabi, S. Zinadini, A. Alizadeh, R. Heydari, M. Beygzadeh, S. Ghouzivand, Polyethersulfone membrane enhanced with iron oxide nanoparticles for copper removal from water: application of new functionalized Fe_3O_4 nanoparticles, Chem. Eng. J., 263 (2015) 101–112.
[26] S. Kamari, F. Ghorbani, Synthesis of magMCM-41 with rice husk silica as cadmium sorbent from aqueous solutions: parameters' optimization by response surface methodology, Environ. Tech., 38 (2017) 1562–1579.
[27] K. Wantala, S. Sthiannapkao, B.-O. Srinameb, N. Grisdanurak, K.W. Kim, Synthesis and characterization of Fe-MCM-41 from rice husk silica by hydrothermal technique for arsenate adsorption, Environ. Geochem. Health, 32 (2010) 261–266.
[28] H.T. Jang, Y.K. Park, Y.S. Ko, J.Y. Lee, B. Margandan, Highly siliceous MCM- 48 from rice husk ash for CO_2 adsorption, Int. J. Greenhouse Gas Control, 3 (2009) 545–549.
[29] S. Kim, E. Marand, I. Junichi, V.V. Guliants, Polysulfone and mesoporous molecular sieve MCM-48 mixed matrix membranes for gas separation, Chem. Mater., 18 (2006) 1149–1155.
[30] S. Kim, E. Marand, High permeability nano-composite membranes based on mesoporous MCM-41 nanoparticles in a polysulfone matrix, Microporous Mesoporous Mater., 114 (2008) 129–136.
[31] B. Zornoza, S. Irusta, C. Tellez, J. Coronas, Mesoporous silica sphere-polysulfone mixed matrix membranes for gas separation, Langmuir, 25(10) (2009) 5903–5909.
[32] M. Valero, B. Zornoza, C. Téllez, J. Coronas, Mixed matrix membranes for gas separation by combination of silica MCM-41 and MOF NH2- MIL-53(Al) in glassy polymers, Microporous Mesoporous Mater., 192 (2014) 23–28.
[33] B.D. Reid, F.A. Ruiz-Trevino, I.H. Musselman, K.J. Balkus, Jr., J.P. Ferraris, Gas permeability properties of polysulfone membranes containing the mesoporous molecular sieve MCM-41, Chem. Mater., 13 (2001) 2366–2373.
[34] R. Schmidt, M. Stocker, D. Akporiaye, E.H. Torstad, A. Olsen, High-resolution electron microscopy and X-ray diffraction studies of MCM-48, Microporous Mater., 5 (1995) 1–7.
[35] B. Boote, H. Subramanian, K.T. Ranjit, Rapid and facile synthesis of siliceous MCM-48 mesoporous materials, Chem. Commun., 43 (2007) 4543–4545.
[36] X. Feng, G. Yang, Y. Liu, W. Hou, J.-J. Zhu, Synthesis of polyaniline/MCM-41 composite through surface polymerization of aniline, J. Appl. Polymer Sci., 101 (2006) 2088–2094.
[37] A.A. Mosafer, M.R. Toosi, M. Asghari, Effect study of hexagonal mesoporous silica/polyaniline nanocomposite on the structural properties of polysulfone membranes and its heavy metal removal efficiency, Sep. Sci. Tech., 52 (2017) 1775–1786.
[38] M.D. Butterworth, R. Corradi, J. Johal, S.F. Lascelles, S. Maeda, S.P. Armes, Zeta potential measurements on conducting polymer-inorganic oxide nanocomposite particles, J. Colloid Interface Sci., 174 (1995) 510–517.
[39] H. Jirankova, J. Mrazek, P. Dolecek, J. Cakl, Organic dye removal by combined adsorption-membrane separation process, Desal. Water Treat., 20 (2010) 96–101.
[40] A.J. Kajekar, B.M. Dodamani, A.M. Isloo, Z. Abdul Karim, N.B. Cheer, A.F. Ismail, S.J. Shilton, Preparation and characterization of novel PSf/PVP/PANI- nanofiber nanocomposite hollow fiber ultrafiltration membranes and their possible applications for hazardous dye rejection, Desalination, 365 (2015) 117–125.
[41] P. Daraei, S.S. Madaeni, N. Ghaemi, M.A. Khadivi, L. Rajabi, A.A. Derakhshan, F. Seyedpour, PAA grafting onto new acrylate-alumoxane/PES mixed matrix nano-enhanced membrane: Preparation, characterization and performance in dye removal, Chem. Eng. J., 221 (2013) 111–123.
[42] G. Zeng, Y. He, Y. Zhan, L. Zhang, Y. Pan, C. Zhang, Z. Yu, Novel polyvinylidene fluoride nanofiltration membrane blended with functionalized halloysite nanotubes for dye and heavy metal ions removal, J. Hazard. Mater., 317 (2016) 60–72.
[43] G. Zeng, Z. Ye, Y. He, X. Yang, J. Ma, H. Shi, Z. Feng, Application of dopamine-modified halloysite nanotubes/PVDF blend membranes for direct dyes removal from wastewater, Chem. Eng. J., 323 (2017) 572–583.
[44] Y. Wang, J. Zhu, G. Dong, Y. Zhang, N. Guo, J. Liu, Sulfonated halloysite nanotubes/polyethersulfone nanocomposite membrane for efficient dye purification, Sep. Pur. Tech., 150 (2015) 243–251.